

Centralized Sliding Mode Control of Power System with UPFC

AMAR HAMACHE and HACHEMI CHEKIREB

Department of Automatics

National Polytechnic School of Algiers

LCP, ENP, 10 Av. Hassen Badi, BP. 182, El-Harrach

ALGERIA

hamache81@yahoo.fr

Abstract: - In this article is proposed a Centralized Sliding Mode Control (CSMC) applied to a UPFC device for controlling power flow and enhancing power system stability. First, we establish a state-space dynamic model of UPFC based on Kirchhoff's equations and (d-q) transformation. This model includes the two voltage source inverters and the DC bus voltage link. Furthermore, in order to cancel the effect of uncertainties which can affect this plant, we develop a centralized version of sliding mode control based on this state model. In the case where the proposed control scheme is used, we simulate the operation of UPFC equipping a High Voltage (HV) electrical line interconnecting two stable nodes. The simulation results show that it is possible and achievable to control the power flow with satisfactory performances regardless of the parameter uncertainties affecting the model plant.

Key-Words: - FACTS, UPFC, Electrical Power System, Real Power, Reactive Power, Sliding Mode Control, Lyapunov Function.

1 Introduction

It is well established that some technical and optimization problems in the system AC grid can be solved by FACTS devices (Flexible AC Transmission Systems). Among them, UPFC (Unified Power Flow Controller) is the device which can realize the FACTS concept more efficiently [1, 2]. It can be used to steady-state power flow control [3, 4], improve power system stability [5-7] and damp out the power swings during transient period [8-10]. Currently, American Electric Power (AEP) has installed a 160-MVA UPFC at the Inez substation in eastern Kentucky, which is the first practical implementation in the world.

Beside, the UPFC operates mainly in the case of load flow control during dynamic and transient conditions that needs for fast response time bellow 100 ms [1, 2, 11-28]. This fast response can be achieved since power electronic equipments are used and supported by sophisticated control laws [1, 2]. This explains the significant interest of the researchers to the concept of UPFC initially introduced by Hingorani [2]. Many papers were devoted to linear control of UPFC such as PI-based control [11-18], SVD control [19, 20] and optimal control [21]. However, in the majority of these articles, the synthesis of controller results from an approximate model of the UPFC where some significant interactions were simply ignored (effect

of the coupling between the STATCOM and the SSSC...).

Moreover, the provided results of PI-based control of UPFC are not very realistic, because generally they are obtained in the absence of parametric variations affecting the system unavoidably.

Little literature was reserved for the nonlinear control of UPFC such as control based on Lyapunov stability theorem [22], adaptive control [23], predictive control [24], feedback linearization control [25-27] and back-stepping control [28]. Moreover, these nonlinear controls were tested by using an incomplete model of UPFC. Indeed, the PWM voltages provided by the STATCOM and the SSSC were represented by sinusoidal voltage sources and the interaction between the two converters was quite simply ignored.

In order to improve the points brought up above, in this paper a more realistic state-space model of the UPFC taking into account the interactions between the various elements of the UPFC is developed. Moreover, a sliding mode control which exhibits a good robustness with respect to internal and external disturbances, as it is well known, is synthesized.

In this paper, we foremost derive, in (d-q) reference frame, a state-space model of the UPFC. This model incorporates the interaction between the STATCOM and SSSC converters. Besides, we propose a new controller of UPFC using adaptive

sliding mode technique and based on its (d-q) state model. The developed control law must conduct to a decoupled control of the power flow and must remain robustness against the effect of uncertainties in system parameters.

In order to achieve this work, the remaining sections of this paper are organized as follows: Section 2 describes shunt and series branches model of UPFC in the state-space. In Section 3, adaptive sliding mode based controller is developed and simulation results in a typical two bus system are carried out in Section 4. Eventually, Section 5 provides some concluding results.

2 Modeling of UPFC

The UPFC is the most sophisticated FACTS system, proposed by Laszlo GYUGYI [1, 2, 20, 28]. It consists, as shown in Figure 1, of two back-to-back Gate Turn-Off Thyristor (GTO) based voltage source inverters (VSIs) sharing a common DC storage capacitor C . One VSI called STATCOM is connected, through a shunt transformer T_{sh} , to the transmission line at which, the other VSI (SSSC) is yet connected by using a series transformer T_{se} . The SSSC is utilized to inject a controlled voltage in series with the line and thereby to force the power flow (real and reactive powers) to a desired value. The control of the STATCOM allows supplying, in one hand real power at its DC terminal in order to regulate the DC bus voltage V_c to its reference V_{Cref} and the other hand, the reactive power at its AC terminal to regulate the AC bus voltage V_t to its reference V_{tref} , too.

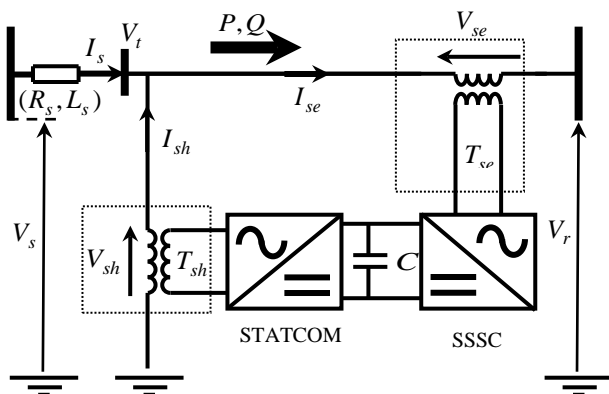


Fig. 1 Basic power system with UPFC

The single-phase scheme representation of three phase transmission system with UPFC is shown in

Fig.2. On this scheme, the series and shunt converters are modeled by the voltage sources V_{sej} and V_{shj} , respectively. Here the subscript j stands for the three-phase quantities (phase a, b and c). The other elements of the scheme are:

- V_{sj} and V_{rj} , the sending and receiving end source voltage;
- L_{sh} and R_{sh} , leakage inductance and resistance of shunt transformer;
- L_{se} and R_{se} , leakage inductance and resistance of the series transformer;
- L_s and R_s , inductance and resistance of the upstream transmission line.

2.1 Series and shunt converters modeling

The mathematical model of shunt and series converters is derived, from the circuit of Fig.2, by applying Kirchhoff's voltage equation. So, currents i_{sh} and i_{se} through the shunt and series paths verify the equations below [27]:

$$(L_s + L_{se}) \frac{di_{sej}}{dt} - L_s \frac{di_{shj}}{dt} = -(R_s + R_{se})i_{sej} + R_s i_{shj} + V_{sj} - V_{sej} - V_{rj} \quad (1)$$

$$L_{se} \frac{di_{sej}}{dt} + L_{sh} \frac{di_{shj}}{dt} = -R_{se} i_{sej} - R_{sh} i_{shj} + V_{shj} - V_{sej} - V_{rj} \quad (2)$$

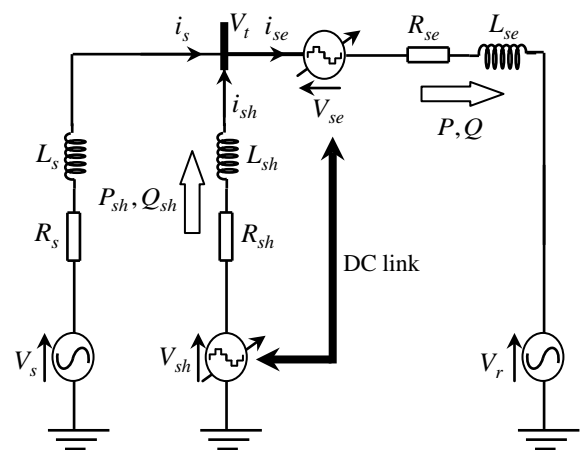


Fig. 2 Single phase equivalent circuit of UPFC

Equations (1) and (2) can be rewritten under the following matrix form:

$$g \frac{d}{dt} \begin{bmatrix} i_{sej} \\ i_{shj} \end{bmatrix} = \begin{bmatrix} a & b \\ c & d \end{bmatrix} \cdot \begin{bmatrix} i_{sej} \\ i_{shj} \end{bmatrix} + \begin{bmatrix} -(\alpha + \beta) & \beta \\ -\beta & \beta + \gamma \end{bmatrix} \cdot \begin{bmatrix} V_{sej} \\ V_{shj} \end{bmatrix} + \begin{bmatrix} \alpha V_{sj} - (\alpha + \beta) V_{rj} \\ -\gamma V_{sj} - \beta V_{rj} \end{bmatrix} \quad (3)$$

where:

$$a = -(R_s L_{sh} + R_{se} L_{sh} + R_{se} L_s), \quad b = R_s L_{sh} - R_{sh} L_s, \\ c = R_s L_{se} - R_{se} L_s, \quad d = -(R_{sh} L_s + R_s L_{se} + R_{sh} L_{se}), \\ g = L_s L_{sh} + L_{se} L_{sh} + L_{se} L_s, \quad \alpha = L_{sh}, \quad \beta = L_s, \quad \gamma = L_{se}.$$

In order to cut down the complexity of the model, the three phase differential equations of the system (1) and (2) are changed into the two-phase equivalent system in the (d-q) reference frame. This rotating (d-q) reference frame is imposed as that the axis (d) is attached to voltage vector V_s . Therefore, the obtained equations, in the (d-q) reference frame, can be put under the following form [18, 20-22]:

$$\dot{\mathbf{X}} = \mathbf{A}\mathbf{X} + \mathbf{B}\mathbf{U} + \mathbf{W} \quad (4)$$

Where \mathbf{X} , \mathbf{U} and \mathbf{W} are the state vector, control vector and residual terms vector, respectively. Vectors \mathbf{X} , \mathbf{U} and \mathbf{W} matrices \mathbf{A} and \mathbf{B} stand for:

$$\mathbf{X} = \begin{bmatrix} i_{sed} \\ i_{seq} \\ i_{shd} \\ i_{shq} \end{bmatrix}, \quad \mathbf{U} = \begin{bmatrix} V_{sed} \\ V_{seq} \\ V_{shd} \\ V_{shq} \end{bmatrix},$$

$$\mathbf{W} = \frac{1}{g} \begin{bmatrix} \alpha V_{sd} - (\alpha + \beta) V_{rd} \\ \alpha V_{sq} - (\alpha + \beta) V_{rq} \\ -\gamma V_{sd} - \beta V_{rd} \\ -\gamma V_{sq} - \beta V_{rq} \end{bmatrix},$$

$$\mathbf{A} = \frac{1}{g} \begin{bmatrix} a & g\omega & b & 0 \\ -g\omega & a & 0 & b \\ c & 0 & d & g\omega \\ 0 & c & -g\omega & d \end{bmatrix},$$

$$\mathbf{B} = \frac{1}{g} \begin{bmatrix} -(\alpha + \beta) & 0 & \beta & 0 \\ 0 & -(\alpha + \beta) & 0 & \beta \\ -\beta & 0 & \beta + \gamma & 0 \\ 0 & -\beta & 0 & \beta + \gamma \end{bmatrix}.$$

Here, $\omega = 2\pi f$ is the pulsation of the AC grid with the fundamental frequency $f = 50$ Hz.

2.2 DC link modeling

It is well established that the operation of the UPFC is strongly related to the stability of the DC bus voltage [12, 22, 24, 26, 28]. In order to build up, in the sequel, a DC voltage regulation, an adequate model of the DC link must be available. Fig. 3 shows an approximate equivalent circuit, where the resistor R emulates the losses related to the electronic power components of the UPFC system. This model is based on the balance of the instantaneous power between the AC side power and the DC side power of the converters.

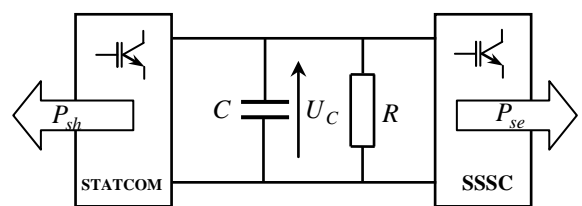


Fig. 3 DC voltage circuit of UPFC

As the stored energy E in a capacitor is $E = \frac{1}{2} C U_c^2$, hence, the energy balance gives right to write:

$$\frac{dE}{dt} = -(P_{sh} + P_{se} + \frac{U_c^2}{R}) \quad (5)$$

Where P_{sh} and P_{se} are the real powers injected into the AC bus respectively by the STATCOM and the SSSC. They are given by the following expressions [19]:

$$\begin{cases} P_{sh} = V_{shd} i_{shd} + V_{shq} i_{shq} \\ P_{se} = V_{sed} i_{sed} + V_{seq} i_{seq} \end{cases} \quad (6)$$

Equation (5) can be written as

$$\frac{dU_c^2}{dt} = -\frac{2}{C} \left(P_{sh} + P_{se} + \frac{U_c^2}{R} \right) \quad (7)$$

The above equation gives the dynamic model of the DC bus voltage.

3 UPFC Control System

3.1 Control Scheme

Control scheme applied for the UPFC system appears in Fig. 4 where, the regulation of the DC and AC bus voltages conducts to the references (P_{shref}, Q_{shref}) of active and reactive powers related to the STATCOM. Moreover, the reference values (P_{ref}, Q_{ref}) of real and reactive powers at the receiving end are forced by the SSSC and they are usually specified by the coordinating system controller in such transmission AC grid.

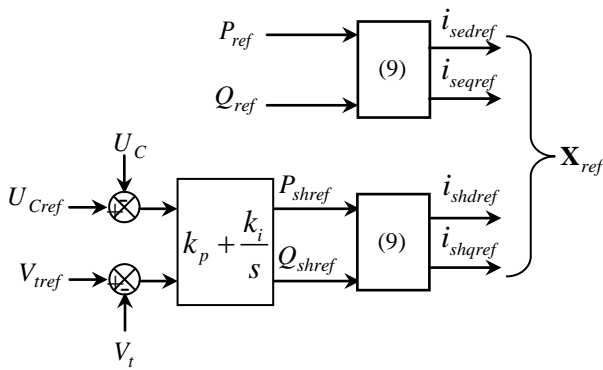


Fig. 4 Current reference values calculation for UPFC controller

In the (d-q) axis, the instantaneous real and reactive powers P and Q are given by [15, 18, 19, 24]:

$$\begin{cases} P = V_{rd}i_d + V_{rq}i_q \\ Q = V_{rq}i_d - V_{rd}i_q \end{cases} \quad (8)$$

Resolving equation (8) for currents, we obtain the expression bellow:

$$\begin{cases} i_d = \frac{PV_{rd} + QV_{rq}}{V_{rd}^2 + V_{rq}^2} \\ i_q = \frac{PV_{rq} - QV_{rd}}{V_{rd}^2 + V_{rq}^2} \end{cases} \quad (9)$$

2.2 Centralized Sliding Mode Control (CSMC) of UPFC

It is clear that parameters of the plant are corrupted by uncertainties and variations and especially we are interested to those affecting the vector \mathbf{W} which includes terms depending of distant and delayed measurements. In this case, it would be attractive to design a robust controller against the parameter uncertainties. Using CSMC technique, we intend to design a robust controller for this plant which guarantees fast and stable regulation under all operating conditions and parameter variations.

We assume that the nominal value \mathbf{W}_n of \mathbf{W} is well known and that $\Delta\mathbf{W}$ is its uncertainty which is given by $\Delta\mathbf{W} = [\Delta w_1 \ \Delta w_2 \ \Delta w_3 \ \Delta w_4]^T$.

Consider the following positive definite Lyapunov function candidate [29]:

$$\mathbf{V} = \frac{1}{2} \mathbf{S}^T \mathbf{S} \quad (10)$$

Where $\mathbf{S} = \mathbf{X} - \mathbf{X}_{ref}$ is a sliding mode surface vector corresponding to the current tracking error.

Differentiating \mathbf{V} with respect to time gives

$$\dot{\mathbf{V}} = \mathbf{S}^T (\dot{\mathbf{X}} - \dot{\mathbf{X}}_{ref}) \quad (11)$$

First, we consider only the nominal value \mathbf{W}_n . Substituting in (11), $\dot{\mathbf{X}}$ by its expression (4) conducts to

$$\dot{\mathbf{V}} = \mathbf{S}^T (\mathbf{A}\mathbf{X} + \mathbf{B}\mathbf{U} + \mathbf{W}_n - \dot{\mathbf{X}}_{ref}) \quad (12)$$

$\dot{\mathbf{V}}$ is made negative definite by imposing:

$$\dot{\mathbf{S}} = -\mathbf{K}_d \mathbf{S} - \mathbf{K} \text{sign}(\mathbf{S}) \quad (13)$$

where:

$$\begin{cases} \mathbf{K} = \text{diag} ([k_1 \ k_2 \ k_3 \ k_4]), k_i > 0, i = 1, \dots, 4; \\ \mathbf{K}_d = \text{diag} ([k_{d1} \ k_{d2} \ k_{d3} \ k_{d4}], k_{di} > 0, i = 1, \dots, 4; \\ \text{sign}(\mathbf{S}) = [\text{sign}(s_1) \ \text{sign}(s_2) \ \text{sign}(s_3) \ \text{sign}(s_4)]^T \end{cases}$$

Thus, we can write

$$\mathbf{A}\mathbf{X} + \mathbf{W}_n + \mathbf{B}\mathbf{U} - \dot{\mathbf{X}}_{ref} = -\mathbf{K}_d \mathbf{S} - \mathbf{K} \text{sign}(\mathbf{S}) \quad (14)$$

Since the matrix \mathbf{B} is invertible, the control law is deduced from (14), it is given by

$$\mathbf{U} = \mathbf{B}^{-1} (\dot{\mathbf{X}}_{ref} - \mathbf{A}\mathbf{X} - \mathbf{W}_n - \mathbf{K}_d \mathbf{S} - \mathbf{K} \text{sign}(\mathbf{S})) \quad (15)$$

and $\dot{\mathbf{V}}$ is reduced to $\dot{\mathbf{V}} = -\mathbf{K}_d \mathbf{S} - \mathbf{K} \text{sign}(\mathbf{S})$.

Thus, we can write

$$\dot{V} = -\sum_{i=1}^4 k_{di} s_i^2 - \sum_{i=1}^4 k_i |s_i| \quad (16)$$

From (16), we obtain $\dot{V} < 0 \quad \forall s_i \neq 0$, which means that s_i is bounded and converges asymptotically toward zero. So, the current vector \mathbf{X} tracks the desired trajectory \mathbf{X}_{ref} .

The UPFC control system which is based on the control law in (15) is represented in fig.5.

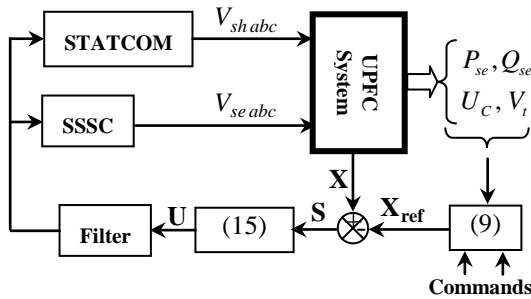


Fig. 5 UPFC control system scheme

Now, we have to introduce the uncertainty $\Delta \mathbf{W}$, so we can write

$$\mathbf{W} = \mathbf{W}_n + \Delta \mathbf{W} \quad (17)$$

In addition, this uncertainty is assumed to be bounded, it means that $\forall t > 0: \exists \Delta \bar{w}_i > 0$ such as

$$|\Delta w_i| < \Delta \bar{w}_i, i = 1..4 \quad (18)$$

Consider the positive definite Lyapunov function candidate in (10) and the expression of \mathbf{W} in (17), (14) can be written as

$$\mathbf{A}\mathbf{X} + \mathbf{W}_n + \Delta \mathbf{W} + \mathbf{B}\mathbf{U} - \dot{\mathbf{X}}_{ref} = -\mathbf{K}_d \mathbf{S} - \mathbf{K} \text{sign}(\mathbf{S}) \quad (19)$$

Substituting in (19), the control \mathbf{U} by its expression (15) conducts to

$$\dot{V} = \mathbf{S}^T (-\mathbf{K}_d \mathbf{W} - \mathbf{K} \text{sign}(\mathbf{S}) - \dots) \quad (20)$$

After developing, (20) takes the form

$$\dot{V} = -\sum_{i=1}^4 k_{di} s_i^2 - \sum_{i=1}^4 k_i |s_i| - \sum_{i=1}^4 \Delta w_i s_i \quad (21)$$

This can be bounded as

$$\dot{V} \leq -\sum_{i=1}^4 k_{di} s_i^2 - \sum_{i=1}^4 k_i |s_i| + \sum_{i=1}^4 \Delta \bar{w}_i |s_i| \quad (22)$$

The inequality above leads to

$$\dot{V} \leq -\sum_{i=1}^4 k_{di} s_i^2 - \sum_{i=1}^4 (k_i - \Delta \bar{w}_i) |s_i| \quad (23)$$

To make \dot{V} negative definite, a suitable choice for k_i is:

$$k_i \geq \Delta \bar{w}_i, i = 1..4 \quad (24)$$

In this case,

$$\dot{V} \leq -\sum_{i=1}^4 k_{di} s_i^2 \quad (25)$$

We know that there exists a centroid coefficient $k_b > 0$ such that $\sum_{i=1}^4 k_{di} s_i^2 = k_b \sum_{i=1}^4 s_i^2$, and (25) can be rewritten as:

$$\dot{V} \leq -k_b \sum_{i=1}^4 s_i^2 \quad (26)$$

So,

$$\dot{V} \leq -k_b V \quad (27)$$

This makes

$$0 \leq V(t) \leq V(0)e^{-k_b t} \quad (28)$$

The expression (28) means that all electrical sizes are bounded and the tracking error \mathbf{S} converges exponentially toward zero.

4 Simulation and Interpretation

In this section, we intend to simulate the operation of power AC transmission line equipped with UPFC. These simulations are carried out when the UPFC is driven by the proposed control law in the case of a HV interconnection 400 kV - 50 Hz of 200 km long with a capacity of 800 MVA. This interconnection is assumed to link two stable electrical nodes characterized by the same amplitude voltages and a transmission phase angle δ of 10°. The UPFC impedances in Fig. 2 are given in Table 1. The voltage and power ratings are 400 kV and 1000 MVA, respectively.

The STATCOM and SSSC are multilevel converters of five levels and which are controlled using a PWM technique with triangular carrier of 1 kHz frequency.

Table 1 The UPFC parameters (in p.u)

$R_s + j\omega L_s$	$R_{sh} + j\omega L_{sh}$	$R_{se} + j\omega L_{se}$	$\frac{1}{\omega C}$
0.058 + j0.630	0.025 + j0.625	0.012 + j0.004	0.004

The main objectives of UPFC system are [24]:

- Controlling real and reactive powers (P, Q) exchanged between the two nodes;
- Maintaining the rms value of the shunt connection node V_i close to 400 kV;
- Regulating DC link voltage U_c to its reference value $U_{Cref} = 40$ kV.

The simulations are started with initial conditions related to the considered interconnection (without UPFC) operating at the following steady-state: $P = 267$ MW, $Q = -62$ MVar and $V_s = V_r = 400$ kV.

It should be noted that a low pass filter with a suitable cutoff frequency $f_c = 300$ Hz is necessarily placed after the sign function to reduce the chattering phenomena.

For CSMC, the satisfying results are carried out with control coefficients imposed as follows:

$$\mathbf{K} = 10^4 \text{diag}([1 \ 1 \ 1 \ 1]), \mathbf{K}_d = 10^4 \text{diag}([1 \ 1 \ 1 \ 1])$$

From Fig. 6, Fig. 7 and Fig. 8, it is obvious that the proposed Controller has allowed realizing the tracking references of the real and reactive powers with a good precision at the receiving end of the interconnection line. The same figures reveal similarly that the shunt node voltage V_i is stabilized around its reference value with a maximum error of 7%.

Moreover, the injected voltage by the SSSC and the injected current by the STATCOM remain in the realistic range for the level rating of this considered power AC line. Noticing that the CSMC ensures good decoupling action between the control of real and reactive powers in perturbed case since the disturbance is rejected in 50 ms.

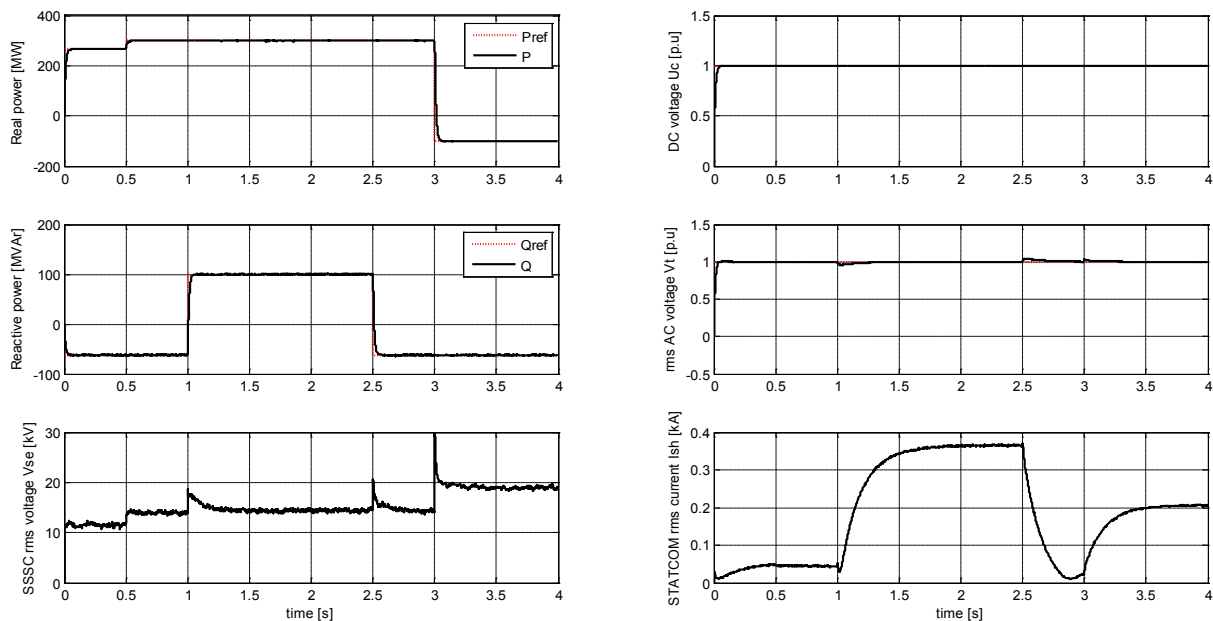


Fig.6 System response in ideal case (without parameter uncertainties)

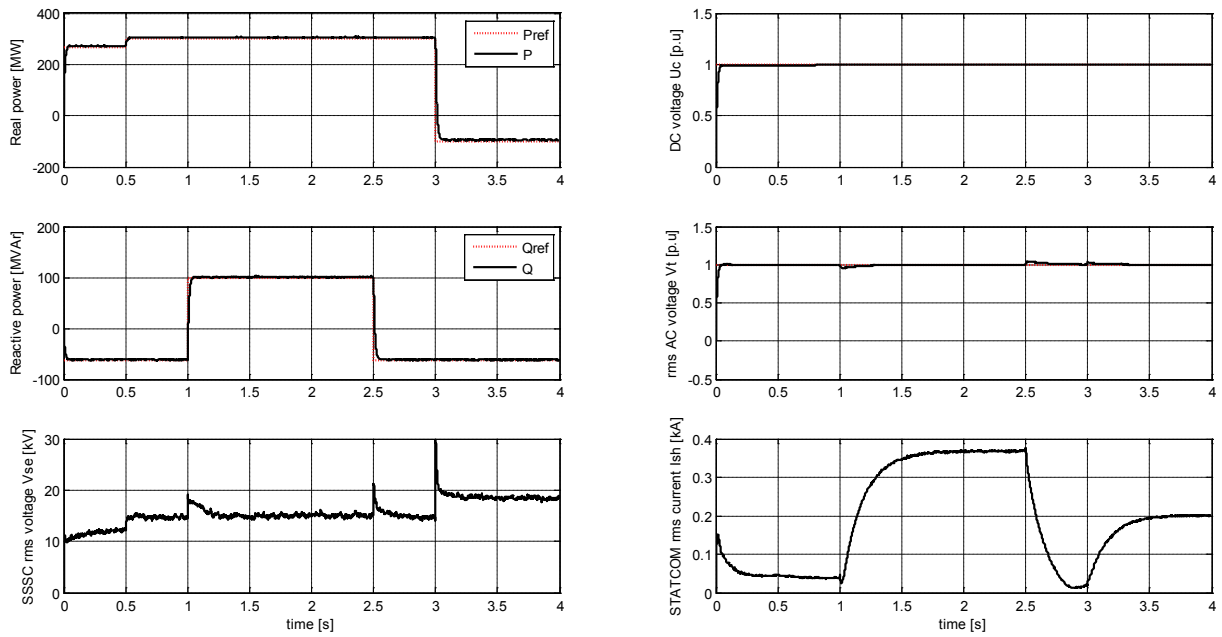


Fig.7 System response with 40% parameters uncertainty

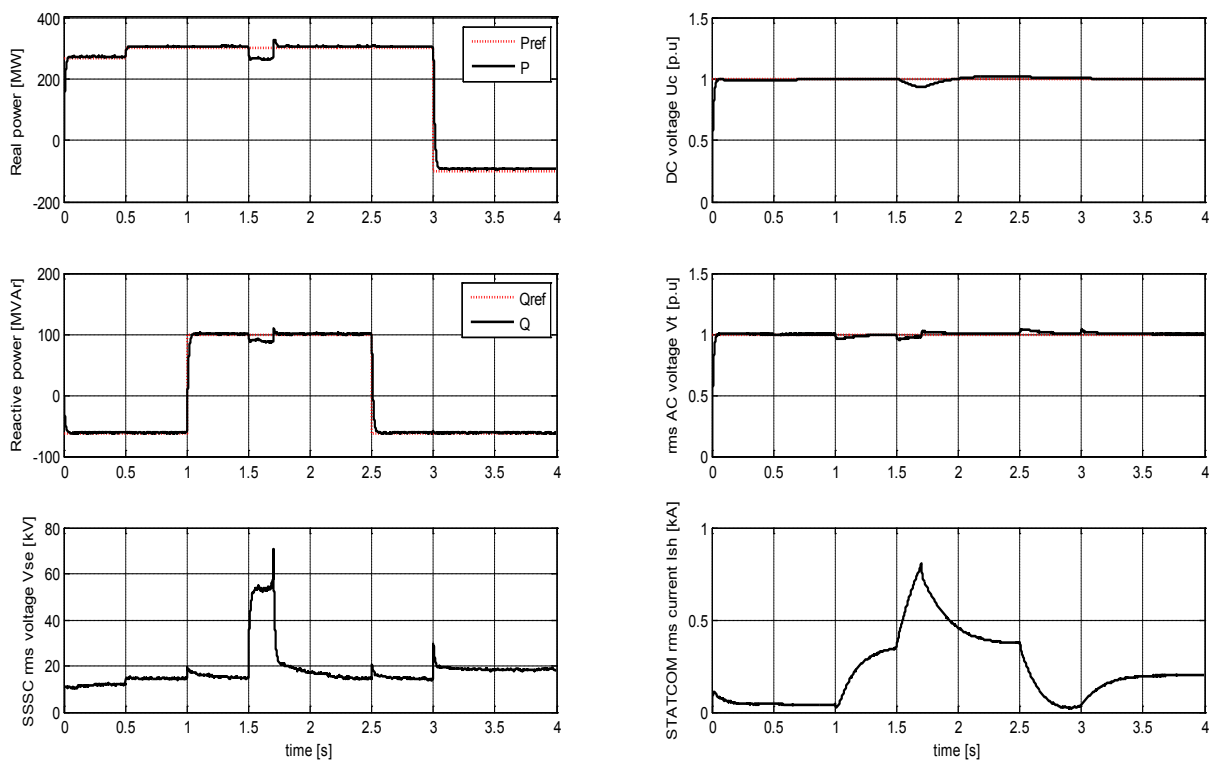


Fig.8 System response to a voltage sag of 60% at 1.5 s for 200 ms and 20% parameters uncertainty

5 Conclusion

The objective of this work is to synthesize a CSMC to drive an UPFC plant in order to control the real and reactive powers at the receiving end of the AC power line and to regulate the voltage at its

interconnection node. In this goal, a detailed model of UPFC plant has been developed in state-space which has been utilized in order to release a CSMC law. The simulations are carried out when the proposed control law is applied in the case of a HV interconnection 400 kV - 50 Hz of 200 km long

with a capacity of 800 MVA. The obtained results show that an absolute decoupled and bidirectional power flow are attained. In addition, the CSMC scheme is seen to be robust against parameters uncertainties, high frequencies due to PWM techniques and external AC voltage disturbances.

The proposed approach has simple structure and quick performance in comparison with robust intelligent methods such as fuzzy sets, neural networks or genetic algorithms. Thus, the results validate the effectiveness of the scheme for the independent control of real and reactive power flows.

References:

- [1] D. Povh et al., Load Flow Control in High Voltage Systems Using Facts Controllers, *CIGRE TF 38-01-06 on Load Flow Control, SIEMENS*, October 1995.
- [2] N. G. Hingorani and L. Gyugyi, *Understanding FACTS: Concepts and Technology of Flexible AC Transmission Systems*, New York IEEE Press, 2000.
- [3] Q. Tong and Q. Jiang, A novel method of power flow analysis with UPFC considering limit violations of variable, *International Conference on Electric Information and Control Engineering (ICEICE)*, 2011, pp. 70-74.
- [4] A. L. Ara, A. Kazemi and S. A. N. Niaki, Modelling of Optimal Unified Power Flow Controller (OUPFC) for Optimal Steady-State Performance of power Systems, *Energy Conversion and Management*, Vol. 52, 2011, 1325-1333.
- [5] R. Tiwari, K. R. Niazi and V. Gupta, Decoupled Power Exchange Model of UPFC to Enhance Voltage Stability Margin of Power Systems, *IEEE Power and Energy Society General Meeting*, 2011, pp. 1-8.
- [6] M. E. Elgamal, A. Lotf and G. E. M. Ali, Voltage Profile Enhancement by Fuzzy Controlled MLI UPFC, *Electrical Power and Energy Systems*, Vol. 34, 2012, pp. 10-18.
- [7] M. J. Kumar, S. S. Dash, A. S. P. Immanuel and R. Prasanna, Comparison of FBLC (Feed-Back Linearisation) and PI-Controller for UPFC to Enhance Transient Stability Computer, *International Conference on Communication and Electrical Technology (ICCET)*, 2011, pp. 376-381.
- [8] L. H. Hassan, M. Moghavvemi, H. A. F. Almurib, K. M. Muttaqi and H. Duc, Damping of Low-Frequency Oscillations and Improving Power System Stability via Auto-Tuned PI Stabilizer using Takagi–Sugeno Fuzzy Logic, *Electrical Power and Energy Systems*, Vol. 38, 2012, pp. 72-83.
- [9] S. A. Taher, R. Hemmati, A. Abdolalipour and S. Akbari, Comparison of Different Robust Control Methods in Design of Decentralized UPFC Controllers, *Electrical Power and Energy Systems*, Vol. 43, 2012, pp. 173-184.
- [10] Anju Gupta, P. R. Sharma, Static and Transient Voltage Stability Assessment of Power System by Proper Placement of UPFC with POD Controller, *WSEAS Transactions on Power Systems*, Vol. 8, No. 4, October 2013, pp. 197-206.
- [11] L. Dong, M. L. Crow, Z. Yang, C. Shen, L. Zhang and S. Atcitty, A Reconfigurable FACTS System for University Laboratories, *IEEE Trans. Power Systems*, vol. 19, No. 1, April. 2004, pp. 120-128.
- [12] Y. L. Kang, G. B. Shrestha and T. T. Lie, Consideration of DC Capacitor and Line Inductance in the Design of UPFC to Improve Transient Stability, *IEEE Power Engineering Society Winter Meeting*, Vol. 3, 2001, pp. 1277-1282.
- [13] P. Zhu, L. Liu, X. Liu, Y. Kang and J. Chen, "Analysis and Comparison of two Control Strategies for UPFC, *Transmission and Distribution Conference and Exhibition: Asia and Pacific, IEEE/PES*, 2005, pp. 1-7.
- [14] L. Xu and V. G. Agelidis, A Flying Capacitor Multilevel Converter Based UPFC, *IEE Proceedings Electric Power Applications*, Vol. 149, No. 4, 2002, pp. 304-310.
- [15] Q. Yu, S. D. Round, L. E. Norum and T. M. Undeland, Dynamic Control of a Unified Power Flow Controller, *Power Electronics Specialists Conference, PESC '96 Recor., 27th Annual IEEE*, Vol. 1, 1996, pp.508-514.
- [16] S. Baskar, N. Kumarappan and R. Gnanadass, Power quality analysis and mitigation case study using Unified Power Flow Controller, *International Conference on Power Electronics (IICPE), India*, 2011, pp. 1-4.
- [17] M. Kang and J. Kim, A real-time control system for single-phase unified power flow controllers, *Electrical Engineering (Archiv fur Elektrotechnik)*, Vol. 91, 2010, pp. 439-450.
- [18] S. L. L. Lima, E. H. Watanabe, UPFC based on single-phase converters for voltage control, *Power Electronics Conference (COBEP)*, 2011, pp. 107-113.

- [19] M. Ghanbari and S. M. Hosseini, Dynamic SVD Controller Design of UPFC for Power Flow Control Considering Interactions, *IEEE International Conference on Industrial Technology ICIT*, 2008, pp. 1-6.
- [20] C. M. Yam and M. H. Haque, A SVD based controller of UPFC for power flow control, *Electric Power Systems Research*, Vol. 70, June 2004, pp. 76-84.
- [21] H. Alasooly and M. Redha, Optimal control of UPFC for load flow control and voltage flicker elimination and current harmonics elimination, *Computers and Mathematics with Applications*, Vol. 60, 2010, pp. 926-943.
- [22] Ali Zangeneh, Ahad Kazemi, Majid Hajatipour and Shahram Jadid, A Lyapunov theory based UPFC controller for power flow control, *Electrical Power and Energy Systems*, Vol. 31, 2009, pp. 302-308.
- [23] M. E. A. Putrus and G. A. Farrag, Design of an Adaptive Neurofuzzy Inference Control System for the Unified Power-Flow Controller, *IEEE Transactions on Power Delivery*, Vol. 27, 2012, pp. 53-61.
- [24] H. I. Shaheen, G. I. Rashed, S. G. Sheng, Design of New Nonlinear Optimal Predictive Controller for Unified Power Flow Controller, *IEEE Power and Energy Society General Meeting, Conversion and Delivery of Electrical Energy in the 21st Century*, 2008, pp. 1-10.
- [25] B. Lu and B. T. Ooi, Nonlinear Control of FACTS and HVDC Belonging to the Voltage-Source Converter family, *IEEE Conference on Control Applications*, 2005, pp. 617-623.
- [26] G. S. Ilango, C. Nagamani, A.V.S.S.R Sai and D. Aravindan, Control algorithms for control of real and reactive power flows and power oscillation damping using UPFC, *Electric Power Systems Research, Region 10 Conference*, Vol. 79, No. 4, April 2009, pp. 595-605.
- [27] G. Saravanailango and C. Nagamani, A Non-linear Control Technique for Unified Power Flow Controller Based on Feed-back Linearization, *Electric Power Components and Systems*, Vol. 36, 2008, pp. 432-447.
- [28] G. S. Ilango, C. Nagamani and D. Aravindan, Independent Control of Real and Reactive Power Flows using UPFC based on Adaptive Back Stepping, *TENCON 2008 - 2008 IEEE Region 10 Conference*, pp. 1-6.
- [29] Sezai Tokat, Serdar Iplikci, Lutfi Ulusoy, Observer Gain Adaptation of Output Feedback Sliding Mode Controller with Support Vector Machine Regression, *WSEAS Transactions on Systems and Control*, Vol. 5, No. 2, February 2010, pp. 112-122.